Mechanics & Industry **17**, 605 (2016)

DOI: 10.1051/meca/2016002
www.mechanics-industry.org

Mechanics & Industry

FE optimization of the ejection force of a spring-maintained connector

Fabien Bogard[1,a], Sébastien Murer[1], Karl Debray[1], Ning Yu[2] and Benoit Bartkowiak[2]

[1] GRESPI/MAN, Université de Reims Champagne-Ardenne, Moulin de la Housse, Reims, France
[2] Axon'Cable, Route de Châlons-en-Champagne, Montmirail, France

Received 9 July 2015, Accepted 8 January 2016

Abstract – The connector studied herein is a self-ejecting microconnector that features a circular compression spring. This type of circular connector ensures reliable connections for systems requiring reduced weight and miniaturization. Being implemented in various military and aerospace applications, the connector is liable to undergo extreme vibratory loadings and shocks; but even in more common applications (medical sensors, power control systems, communications, etc.) the manufacturer has to guarantee that the two ends will remain properly assembled to ensure electrical continuity. The main purpose of this work is to simulate the whole insertion-extraction process using the finite element method (FEM) and to optimize the ejection force required to unplug the connector. The shape of the groove machined on the male part of the connector is investigated, allowing determination of the geometric parameters of interest. Results will provide manufacturers with useful data, which may also help their customers choose their interconnection solution.

Key words: Numerical model / spring / microconnector / optimization / industry

1 Introduction

The use of microconnectors to ensure electrical continuity is prevalent in technical objects of everyday life (computers, automotive, electrical appliances, etc.), but also in high technology applications, whether military, medical, aerospace or navigation systems. The need for reliable connections (i.e retaining electrical interconnection) requires focusing on the design of the parts actually constituting this interconnection. Several designs can be considered in order to maintain the male and female parts of a connector attached [1–7]. Our case of interest features a spring that tilts as the male connector is pushed through, and recovers its initial shape as it faces a groove machined on the outer surface of the male connector. Thus, relative axial translation is properly blocked between male and female parts of the microconnector. For further reference, components will be referred to as Female-Base, Male-Body, spring, Electric-inserts (Fig. 1). Geometries of all parts have been simplified: for the purpose of reducing the computational cost of the FE model, details having negligible influence on the extraction mechanism have been removed.

[a] Corresponding author:
fabien.bogard@univ-reims.fr

The main concern during the modeling stage was how to take the stressed state of the spring into account. Indeed, a manual operation is required to place it in the appropriate housing: using a pair of pliers and industrial know-how, the technician turns the spring inside out and then places it inside the housing. In the process, the spring undergoes an unquantifiable stress field, which unfortunately cannot be accounted for in the numerical model. Nevertheless, we present a methodology allowing us to simulate this stage. The adopted solution lies in pushing the spring all the way down to its housing.

2 Details about the finite element model

An additional part was created in the form of a fictitious piston used to push the spring into its housing, as seen in Figure 2. This setup yields a more natural placement of the spring, leading to a more realistic stress state.

The next simulation steps consist in pushing the Male-Body through the spring (insertion stage), and then in extracting it while measuring the axial reaction force.

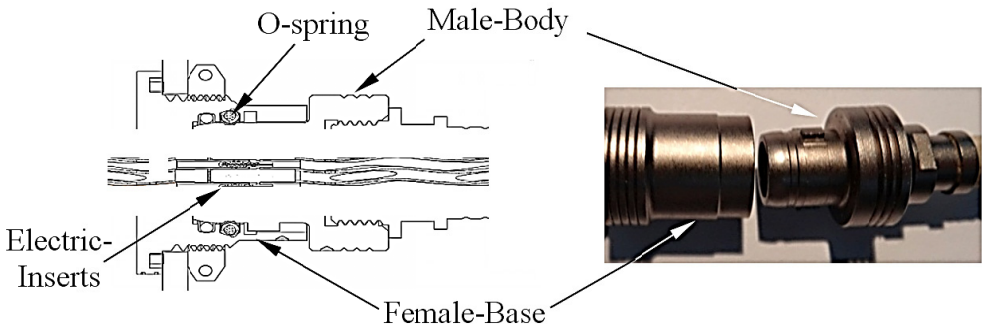

Fig. 1. Self-ejecting microconnector.

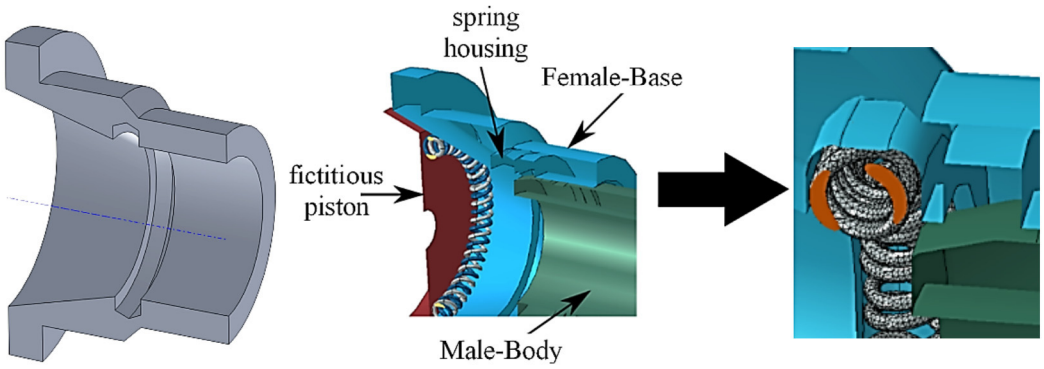

Fig. 2. Cut-view with modified geometry (left), fictitious piston (middle) and spring in place (right).

2.1 Materials and computation steps

The spring is made of an austenitic stainless steel type 302 (Z11CN18-08) with Young's modulus $E = 187\,500$ MPa, Poisson's ratio $\upsilon = 0.31$, coefficient of friction $f = 0.1$ and mass density $\rho = 7920$ kg.m^{-3} [5–9].

In this modeling, both Female-Base and Male-Body will be meshed using rigid R3D4 shell elements (boundaries of these parts are supposed undeformable).

Spring mesh is constituted of deformable tetrahedral C3D4 elements. Depending on the refinement of the spring mesh over several test cases, the total number of elements in the model ranges from 175 000 to 680 000. Our purpose was to achieve the best compromise between results accuracy and computational cost.

2.2 About the electric inserts

Electric inserts must be taken into account due to their significant influence on the value of the extraction force, as shown by an internal technical report [10]. The microconnector was mounted on a tensile testing machine without O-spring, and a series of tests allowed plotting the force-displacement curve displayed in Figure 3.

As seen in Figure 3, an axial force of 30 N is required to take the electric inserts apart: this load adds up to that generated by the spring and cannot be neglected when compared to the extraction force due to the spring alone (i.e. 25 N). Numerically, the inserts will be replaced by a kinematic link named "connector" [11].

The connector is also setup to feature an elastic behavior, as well as a "break" force of 30 N, also derived from experimental results (i.e. axial stiffness of the connector drops to 0 as soon as axial force reaches 30 N), Figure 4.

2.3 Simulation steps

- Spring placement (Fig. 5).
  Spring gets pushed into its housing by the fictitious piston.
- Second step: Male-Body advance through spring (Fig. 6).
  Experimental results [10] have shown that the translational speed of the Male-Body has negligible effects on the measured reaction force (during both insertion and extraction stages). A realistic translational speed of 5 mm.s^{-1} was therefore adopted to obtain accurate placement of each part in the model.
- Third step: Male-Body extraction, measurement of the ejection force.
  During this step, the Male-Body part translates at the same speed as in the previous step (i.e. 5 mm.s^{-1}), but in the opposite direction. The value of the ejection force is measured on the reference point of the Female-Base part.

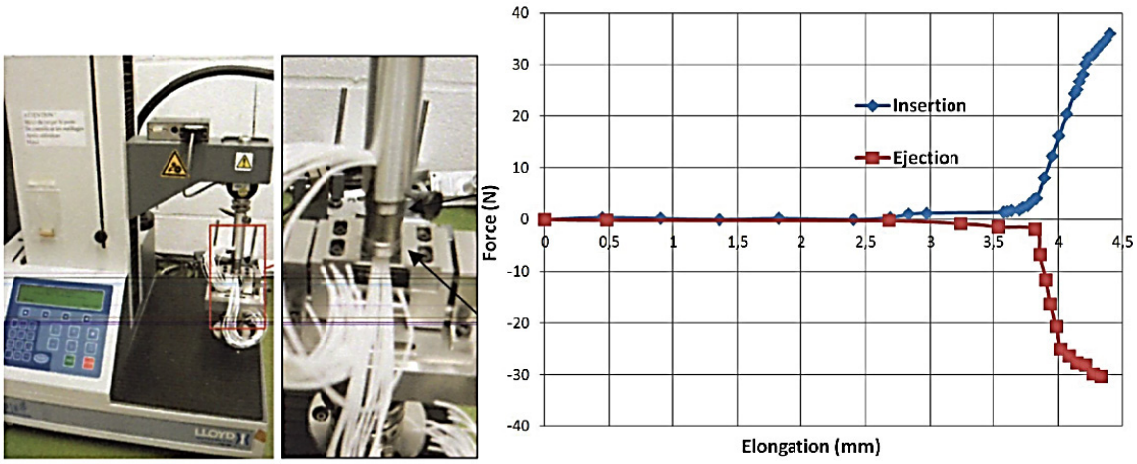

Fig. 3. Experimental measurement of the electric inserts extraction force.

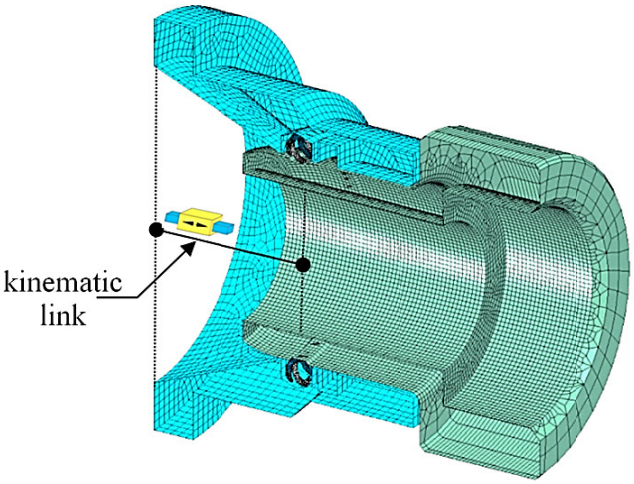

Fig. 4. Kinematic link position between Male-Body and Female-Base.

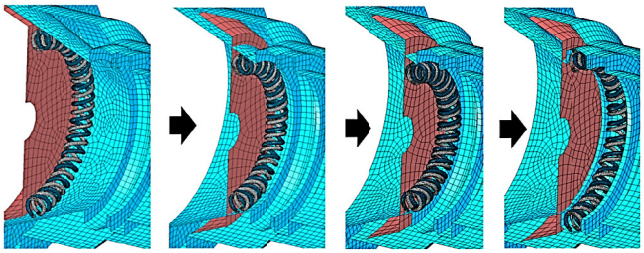

Fig. 5. Spring positioning.

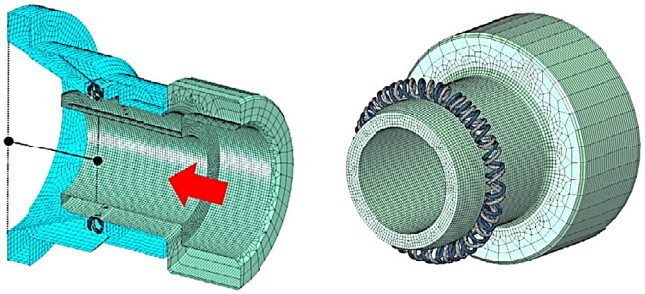

Fig. 6. Advance of Male-Body through O-spring.

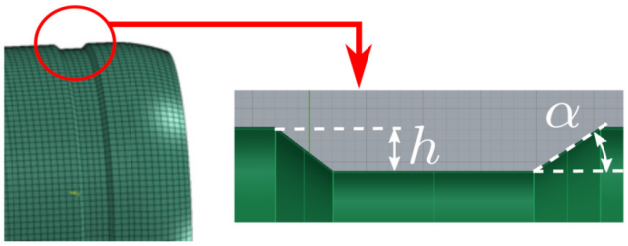

Fig. 7. Geometric details of the groove.

3 Optimization of the connector groove

3.1 Male-Body groove geometry

The geometry of the groove is displayed in Figure 7. The work depicted in this section aims at evaluating the influence of the groove housing the O-spring on the extraction force of the Male-Body part.

Two parameters have been selected in agreement with the manufacturer of the microconnector: groove depth h and slope angle α of the outer end of the groove (i.e. in contact with the O-spring during extraction). Default values read on supplied schematics are $h = 0.15$ mm and $\alpha = 45°$.

3.2 Variation of slope α with $h = 0.15$ mm

Using the new set of parameters, the curve displayed in Figure 8 was plotted.

It appears that the maximal extraction force (87 N) is reached for $\alpha = 90°$ and decreases to 50 N until $\alpha = 50°$, before slightly increasing (54 N) at $\alpha = 45°$ and finally dropping again for $\alpha < 30°$. The increase in the ejection

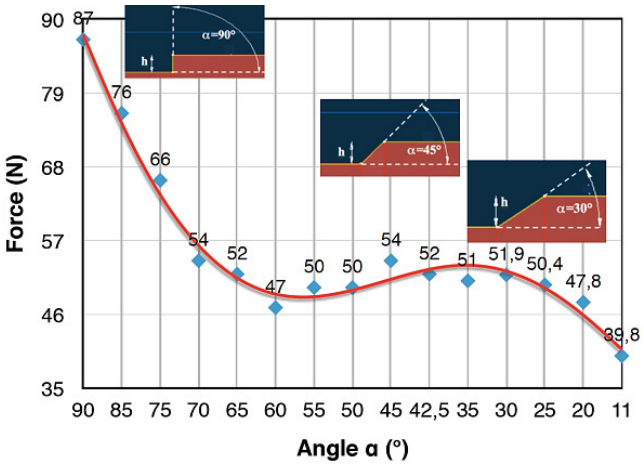

Fig. 8. Ejection force vs. groove slope angle α.

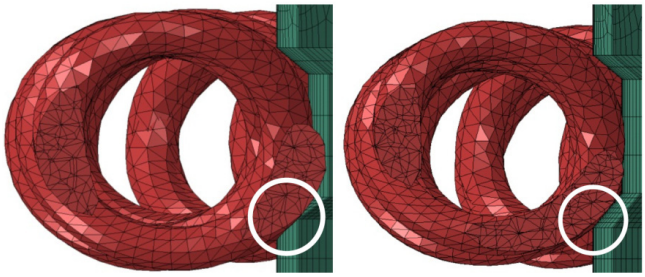

Fig. 9. Slope angle $\alpha = 50°$, contact on edge of groove (left); slope angle $\alpha = 35°$, contact along groove (right).

force for $45° > \alpha > 30°$, although small, highlights a trend which has been observed in all tests.

The explanation could lie in the fact that the contact zone between spring spirals and the Male-Body varies. Indeed, for $\alpha = 50°$ for instance (Fig. 9 left), the O-spring is in contact with the edge of the groove and although slope angle is important, it tilts quite easily out of the groove, requiring a lower extraction effort. When slope angle lies between 45° and 30°, spirals are in contact with the Male-Body on a larger surface (see Fig. 9 right), resulting in a slight increase in the ejection force. If α is set to a value below 35°, slope is insufficient and does not block the spring: the extraction force decreases.

3.3 Variation of groove depth h with $\alpha = 45°$

Another test campaign has been carried out in order to evaluate the consequences of a variation of groove depth h while keeping slope angle α constant. Results are displayed in Figure 10.

For low depths ($h = 0.05$ mm), the extraction force remains small (below 45 N) but it increases along with h, reaching its maximum for $h = 0.15$ mm (initial groove depth) and then decreases, which at first sight may seem counter-intuitive.

This non-linearity in the force vs. h response is actually easily understandable on analyzing cut-views of the

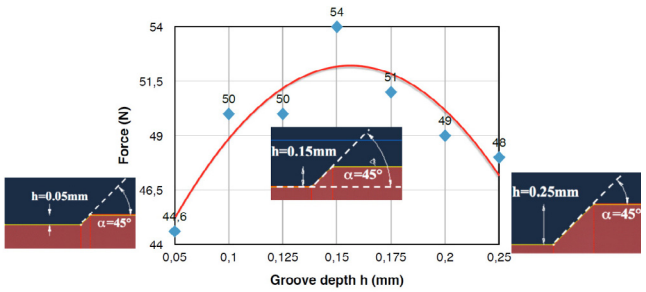

Fig. 10. Ejection force vs. groove depth h.

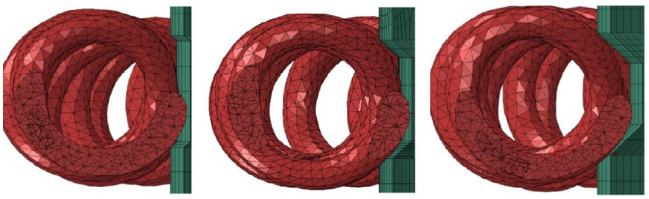

Fig. 11. Spring placement for $h = 0.05$ mm (left), 0.15 mm (middle) and 0.25 mm (right).

spring-groove contact zone with increasing values of h: at some point, contact establishes on the sides of the groove and not at its bottom (Fig. 11 right). Besides, in that case the diameter of the spirals (0.178 mm) is greater than h, thus making spring extraction easier.

3.4 Conclusions on the groove shape

In the light of the results, it appears that the initial geometry of the connector in terms of depth and slope angle of the groove machined in the Male-Body tends to maximize the value of the extraction force.

Yet should a variation of this force be required, modifying the slope angle of the groove seems to be a wise choice, since it has a greater influence on the amplitude of the ejection force. Unfortunately, geometric aspects (spring and spirals diameters) reduce the influence of the groove depth. Nevertheless, slope angle α must be set to a value around 45° due to the previously mentioned non-linearity of the force response.

4 General conclusions and prospects

Intrinsic modeling of the extraction force of a spring-maintained self-ejecting microconnector could not be achieved. Specifics of the spring placement process and the associated stress and strain history were unfortunately not supplied by the manufacturer, preventing us from creating a physically realistic model of the spring behavior.

Despite missing critical information, a parametric study on geometric aspects of the groove housing of the spring has been carried out, highlighting a trend in the evolution of the ejection force as the slope angle of the groove changes. It has been shown that modifying

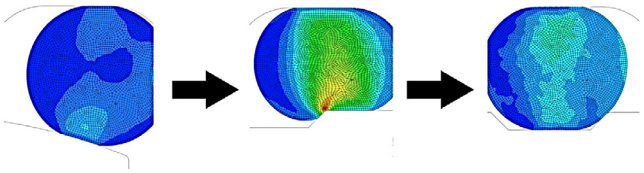

Fig. 12. Preliminary simulation using an elastomeric toroid part instead of the O-spring: Male-Body insertion (left), toroid part entering groove (center), toroid part in position (right).

the slope angle has greater influence on the extraction force than changing the depth of the groove.

As a workaround for the lack of technical data, the O-spring may be replaced by an elastomeric toroid part, the characteristics of which (both geometric and material) being chosen to set the value of the ejection force. Preliminary numerical results are encouraging (Fig. 12).

Acknowledgements. The authors gratefully acknowledge Axon'Cable SAS for technical support and fruitful discussion.

References

[1] M. Buggy, C. Conlon, Material selection in the design of electrical connectors, J. Mater. Process. Technol. 153-154 (2004) 213–218

[2] J. Mackerle, Fastening and joining: finite element and boundary element analyses – A bibliography (1992-1994), Finite Elements in Analysis and Design 20 (1995) 205–215

[3] G. Deal, T. Bernard, Maximum acceptable effort for connector assembly in automotive manufacturing, Int. J. Ind. Ergon. 44 (2014) 207–213

[4] R. Marklin, L. Lazuardi, J. Wilzbacher, Measurement of handle forces for crimping connectors and cutting cable in the electric power industry, Int. J. Ind. Ergon. 34 (2004) 497–506

[5] J.J. Oswald, Modeling of canted coil springs and knitted spring tubes as high temperature seal preload devices, thesis, Case Western Reserve University, 2005

[6] Axon'Cable website, http://www.axon-cable.com

[7] Axon'Cable D-line circular connectors catalogue, 2012

[8] M. Akbarpour, E. Salahi, F.A. Hesari, E. Yoon, H. Kim, A. Simchi, Microstructural development and mechanical properties of nanostructured copper reinforced with SiC nanoparticles, Mater. Sci. Eng. A 568 (2013) 33–39

[9] L. Blaz, Z. Konior, T. Majda, Structural aspects of α/β transformation in hot deformed CuZn-39Pb3 alloy, J. Mater. Sci. 36 (2001) 3629–3635

[10] Y. Zhao, X. Liao, Z. Horita, T. Langdon, Y. Zhua, Determining the optimal stacking fault energy for achieving high ductility in ultrafine-grained Cu-Zn alloys, Mater. Sci. Eng. A 493 (2008) 123–129

[11] X. Wu, X. San, Y. Gong, L. Chen, C. Li, X. Zhu, Studies on strength and ductility of Cu-Zn alloys by stress relaxation, Mater. Design 47 (2013) 295–299

[12] M-Lego website, http://www.m-lego.com

[13] A.C. SAS, Rapport interne, Technical Report, Axon'Cable SAS, 2012

[14] Abaqus 6.12 documentation, 2012